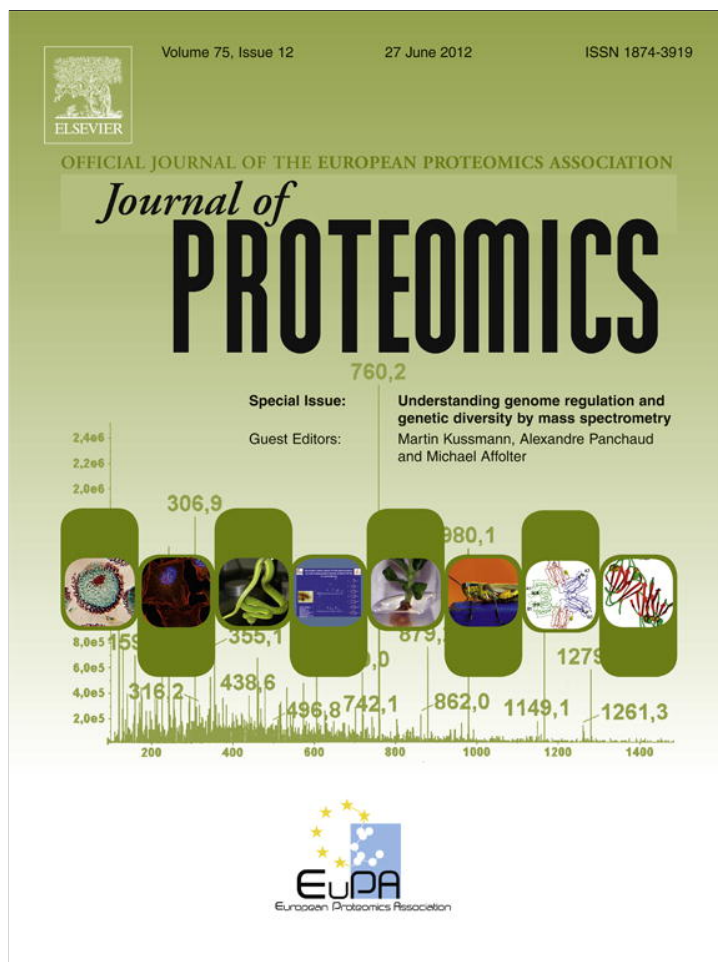


Provided for non-commercial research and education use.
Not for reproduction, distribution or commercial use.



This article appeared in a journal published by Elsevier. The attached copy is furnished to the author for internal non-commercial research and education use, including for instruction at the authors institution and sharing with colleagues.

Other uses, including reproduction and distribution, or selling or licensing copies, or posting to personal, institutional or third party websites are prohibited.

In most cases authors are permitted to post their version of the article (e.g. in Word or Tex form) to their personal website or institutional repository. Authors requiring further information regarding Elsevier's archiving and manuscript policies are encouraged to visit:

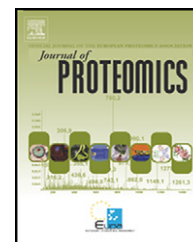
<http://www.elsevier.com/copyright>



ELSEVIER

Available online at www.sciencedirect.com

SciVerse ScienceDirect

www.elsevier.com/locate/jprot

Quantitative proteomic analysis of human osteoblast-like MG-63 cells in response to bioinert implant material titanium and polyetheretherketone

Minzhi Zhao^{a,1}, Mingrui An^{c,1}, Qingsong Wang^c, Xiaochen Liu^a, Wenjia Lai^c, Xuyang Zhao^c, Shicheng Wei^{a,b,*}, Jianguo Ji^{a,c,**}

^aCenter for Biomedical Materials and Tissue Engineering, Academy for Advanced Interdisciplinary Studies, Peking University, Beijing 100871, China

^bCenter for Biomaterials and Medical Devices, School of Stomatology, Peking University, Beijing 100081, China

^cState Key Laboratory of Protein and Plant Gene Research, College of Life Sciences, Peking University, Beijing 100871, China

ARTICLE INFO

Article history:

Received 10 December 2011

Accepted 19 March 2012

Available online 29 March 2012

Keywords:

Biomaterial

Biocompatibility

SILAC

Polyetheretherketone (PEEK)

Titanium

Proteomics

ABSTRACT

Commercially pure titanium (cpTi) and polyetheretherketone (PEEK) are widely used surface-modified implant materials in orthopedics and dental therapeutics. However, there still has not been comprehensive biocompatibility evaluation of them at molecular level. By employing stable isotope labeling with amino acids in cell culture (SILAC), we profiled the dynamic protein expression changes in human osteoblast-like MG-63 cells cultured on cpTi and PEEK, respectively. About 2000 proteins were quantified and 400 proteins showed substantial alterations in expression levels upon each material treatment. Notably, the extent of alterations diminished as the contact prolonged, which suggested adaptive response to the bioinert materials. Similar patterns of expression changes were observed for both cpTi and PEEK. The representative pathways reflected the regulation of biosynthesis, metabolism and cell adhesion in the adaptive process. In addition, PEEK showed stronger inhibition on mRNA processing, which explained the lower proliferation rate of the cells cultured on PEEK. Our results indicated that the widely used bioinert materials cpTi and PEEK could individually induce a cooperative response involving a wide panel of proteins and pathways. This study has established a basis for better understanding the biocompatibility of surface-modified implant biomaterials at molecular level.

© 2012 Elsevier B.V. All rights reserved.

1. Introduction

An in-depth understanding of how cell responding to implant materials is critical for the safety evaluations of biomaterials. The evaluation of biosafety and biocompatibility assessment of biomaterials at the molecular level are seldom studied at

functional proteome level. A systematic proteomics analysis on the biomaterials interacting with their surrounding environmental cells is crucial for the evaluation, application and development of new biomaterials. High-throughput technologies, genomics, transcriptomics and proteomics are being increasingly applied in biomedical studies. Among these technologies, proteomics is

* Correspondence to: S. Wei, Center for Biomaterials and Medical Devices, School of Stomatology, Peking University, Beijing 100081, China. Tel./fax: +86 10 82195780.

** Correspondence to: J. Ji, P.O. Box 31, State Key Laboratory of Protein and Plant Gene Research, College of Life Sciences, Peking University, Beijing 100871, China. Tel.: +86 10 62755470; fax: +86 10 62751526.

E-mail addresses: xgt1986627@163.com (M. Zhao), an5137991@126.com (M. An), wangqingsong@gmail.com (Q. Wang), lxc200107@yahoo.com.cn (X. Liu), wenjia@pku.edu.cn (W. Lai), zhao-xu-yang@163.com (X. Zhao), sc-wei@pku.edu.cn (S. Wei), jjig@pku.edu.cn (J. Ji).

¹ These authors contributed equally to this work.

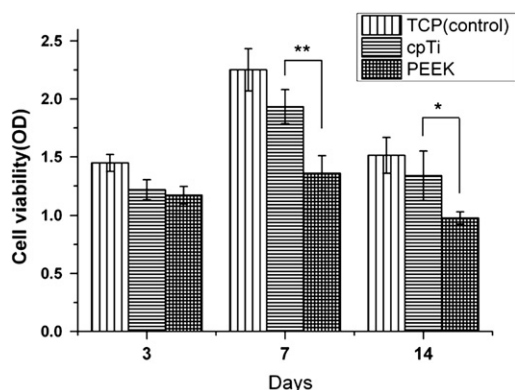


Fig. 1 – Proliferation of cells cultured on TCP, cpTi and PEEK on days 3, 7 and 14 (*: $p < 0.05$; **: $p < 0.001$).

the most important evaluation method [1]. Many recently-developed quantitative proteomic technologies have been gradually introduced to study the cellular dynamic response to biomaterials, such as human osteoblasts cultured on differentially shaped hydroxyapatite nanoparticles [2] and human epidermal keratinocytes exposed to multi-walled carbon nanotubes [3]. Isotope labeling with amino acids in cell culture (SILAC) is an acknowledged metabolic labeling technique which enables the isotopically encoded cells to be mixed before fractionation, thus eliminates inherent quantification biases and achieves more accurate quantitative information[4]. However, this analysis method has not been applied in the protein expression profiling of implant materials that require higher safety standards in clinics. Using SILAC, a highly accurate quantification method, the protein

expression changes can be profiled and the involved signal pathways through which the implant materials interact with the environmental cells can be explored. The biosafety and biocompatibility information of biomaterials at the functional proteome level could also be assessed.

Due to its inertness in the body and high resistance to fatigue, commercially pure titanium (cpTi) is widely used as implant material in orthopedics and dental clinics[5]. Another inert material, polyetheretherketone (PEEK), a partially crystalline polyaromatic linear thermoplastic, was approved as implant material by the U.S. FDA in late 1990s[6]. Elastic modulus of implant materials, which is related to the extent of stress shielding, plays a very important role for repair of bone. Compared to that of many metallic implants, the elastic modulus of PEEK is lower and close to bone [7]. Furthermore, PEEK is an excellent building block for novel biomaterials because of its easy production, natural radiolucency and high resistance to chemicals and sterilization [8]. With good biocompatibility at the cellular level, cpTi usually serves as the direct control for other implant biomaterials.

In this manuscript, we examined the dynamic response of human osteoblast-like MG-63 cells in direct contact with commercially pure titanium (cpTi) and polyetheretherketone (PEEK) on days 3, 7 and 14 through SILAC coupled with mass spectrometry at a whole proteome level. Cells cultured on tissue culture polystyrene (TCP) were selected as the control. Previously, some biomaterials were regarded as biocompatible if they did not induce any obvious adverse or toxic response at the macroscopic and cellular levels. However, moving to the molecular level, more unprecedented physiological phenomena of cells may be observed even upon common inert biomaterials treatment. TCP is usually used for eukaryotic cell culture and most cell lines

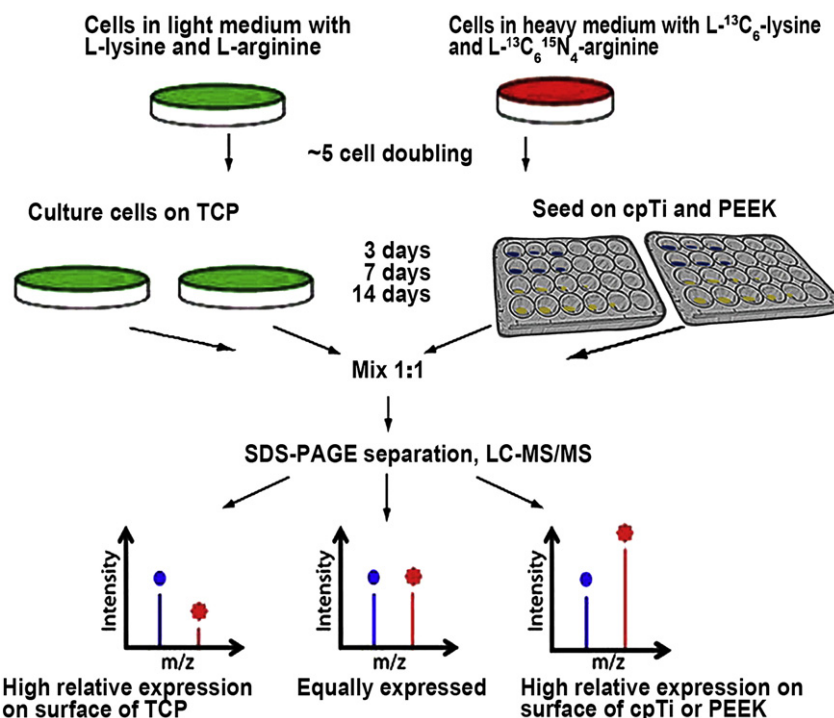


Fig. 2 – Flowchart of SILAC coupled with LC-MS/MS for the comparative analysis of the comparison of protein expression in the MG-63 cells upon different biomaterials treatment. Cells for cpTi and PEEK treatment were completely SILAC-labeled with $^{13}\text{C}_6^{15}\text{N}_4$ -arginine and $^{13}\text{C}_6$ -lysine.

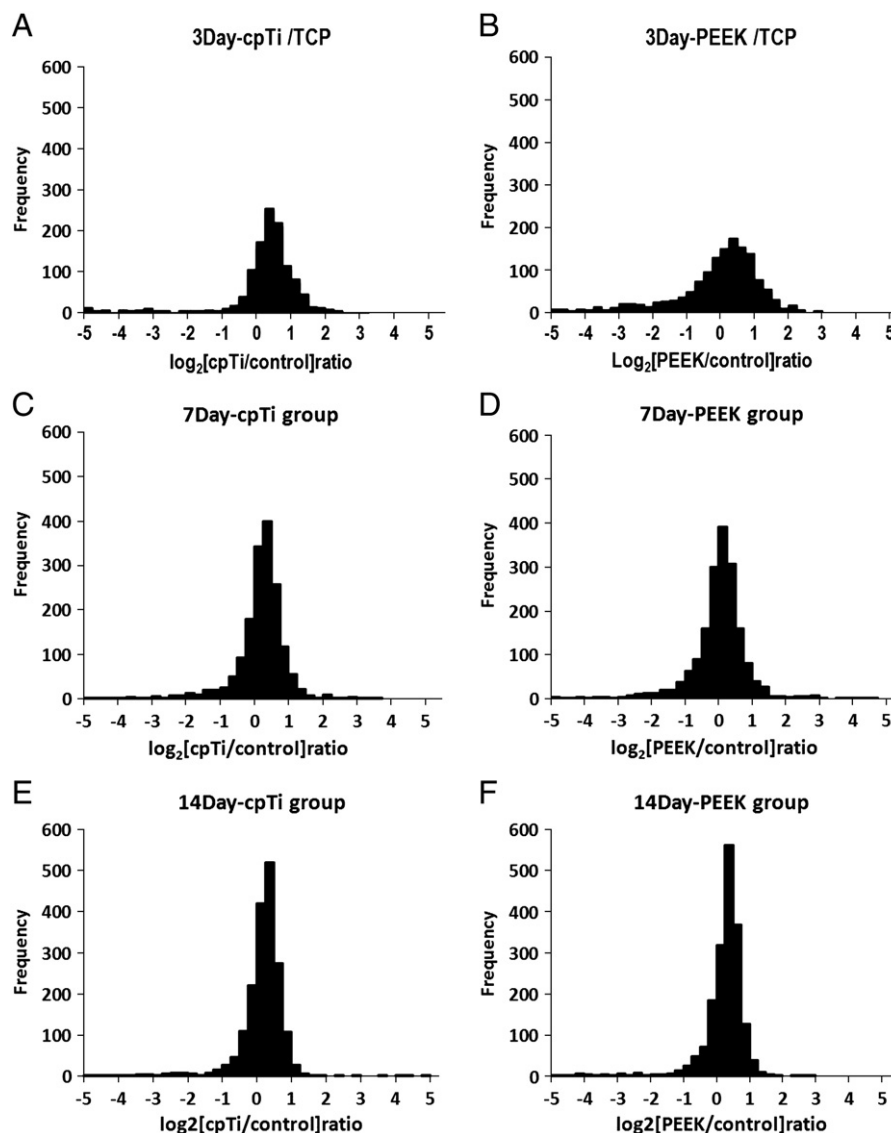


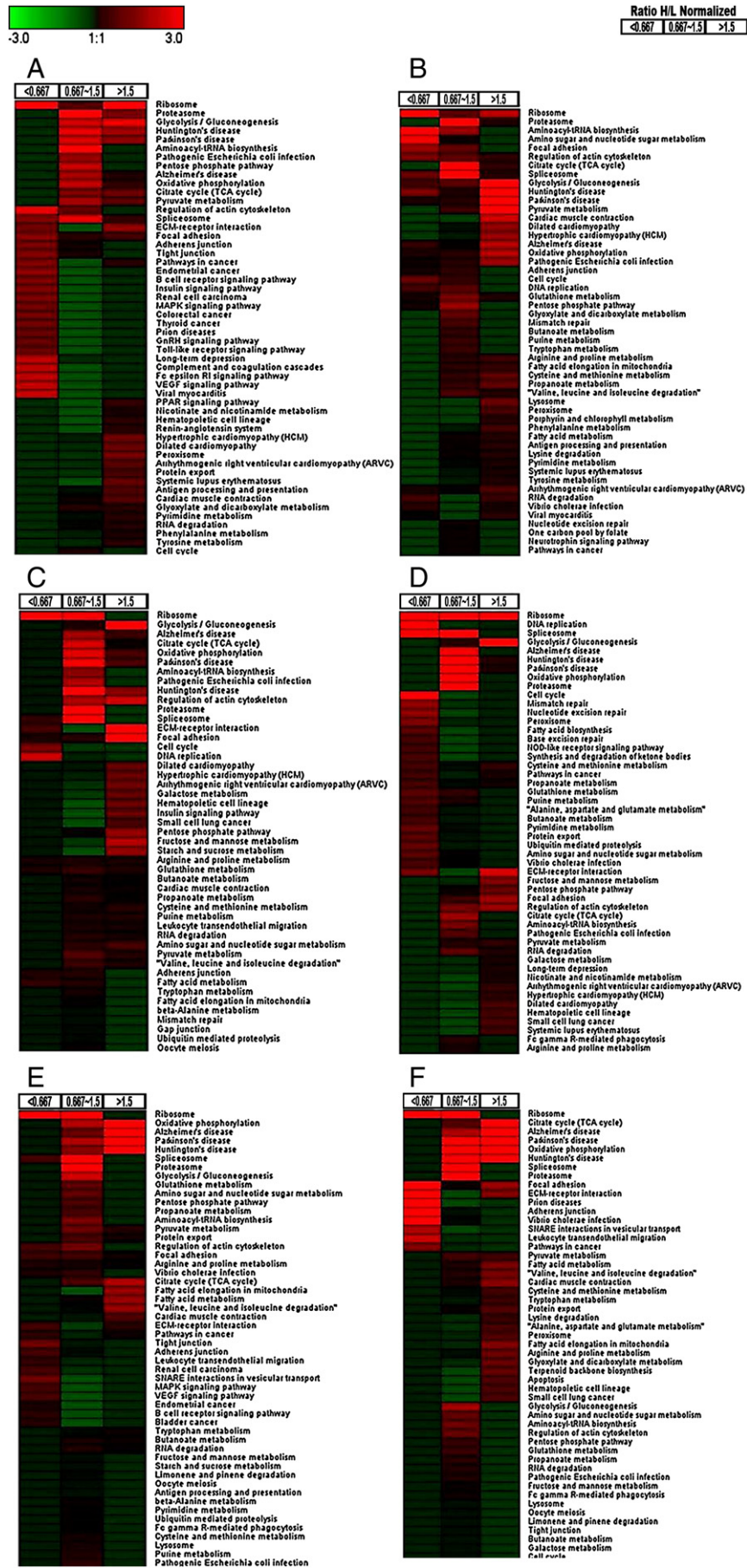
Fig. 3 – Distribution of expression ratios (test material/control) for the quantified proteins. A, C, E, quantitative comparison of the cell proteome in response to cpTi (heavy) and TCP (light) on days 3, 7 and 14. B, D, F, quantitative comparison of the cell proteome response to PEEK (heavy) and TCP (light) on days 3, 7 and 14.

have long been cultured with this material. Therefore, using TCP as control to test cellular responses to changed microenvironments due to the addition of cpTi and PEEK would bring deeper understanding of the safety assessment of the bioinert implant materials on their long application in body.

About 2000 proteins were quantified and about 400 of them showed substantial expression changes. Many proteins changed their expression level after 3, 7 and 14 days of culture. The functions and biological pathways which accommodate expression changes would provide us useful information on the safety and biocompatibility of the implant biomaterials. A systematic

strategy was used for data analysis and interpretation rather than focusing on selected proteins. This strategy was based on two well-established bioinformatics resources: the Kyoto Encyclopedia of Genes and Genomes (KEGG) and the Gene Ontology (GO). Both databases provide standard functional annotations for genes and provide references for proteins, thus supporting high-throughput analyses and providing researchers with clues for the underlying mechanism of biomaterial treatment. Functional enrichment analysis-based hierarchical clustering was utilized for data interpretation. This method is based on an algorithm described previously[9] with minor modifications. It is

Fig. 4 – Functional distributions of proteome comparisons revealed by KEGG pathway analysis. The color bar upright represents the quantiles. A, C, E: representative functional categories of the cell proteomes in response to cpTi against those in response to TCP on days 3, 7 and 14. B, D, F: representative functional categories of the cell proteomes in response to PEEK against those in response to TCP on days 3, 7 and 14.



similar to the clustering of over-represented genes which is frequently employed in microarray-based experiments. With the analysis of the proteins involved biological pathways and networks, the strategy of SILAC coupled with high sensitive LTQ Orbitrap MS identification revealed the regulation information of osteoblast in response to the two widely used implant materials at a global proteome scale.

2. Material and methods

2.1. Material characterizations

Discs of pure Grade 2 titanium (A.D. MacKay, Inc., Red Hook, NY) and implantable grade PEEK (450 G, victrex, Invibio, Thornton Cleveleys, UK), 15 mm in diameter and 2 mm thick were prepared, polished with a series of increasing SiC abrasive papers (80, 400 and 800 grit), and then were ultrasonically cleaned in demineralized water. The surface roughness of cpTi and PEEK samples was measured by a mechanical Dektak8 stylus profiler (TR200, Veeco, Plainview, NY). The surface topography was characterized with an environmental scanning electron microscope (ESEM; Quanta 200FEG, Hillsboro, OR).

2.2. Cell culture, material treatment and scanning electron microscope analysis

Human osteoblast-like MG-63 cells (CRL1427, ATCC, Manassas, VA) were seeded onto the cpTi and PEEK samples in 24-well plates. The control cells were cultured in tissue culture polystyrene (TCP) dishes. The culture medium was Dulbecco's Modified Eagle Medium (DMEM) (Hyclone, Logan, UT) containing 10% (v/v) fetal bovine serum (FBS) (Gibco BRL, Grand Island, NY), penicillin (100 U/ml), and streptomycin sulfate (100 mg/ml). Cells were incubated at 37 °C in a humidified atmosphere with 5% CO₂. After 3, 7, and 14 days of culture, cells on test materials were fixed with 2.5% glutaraldehyde for 60 min at room temperature and then dehydrated through increasing ethanol gradients from 50% to 100%. Cell morphology on materials was examined with an ESEM (Quanta 200FEG). Optical microscopy (Olympus BX 51 M, Japan) was used to observe the morphology of control cells.

2.3. Cell proliferation assay

Cell proliferation reagent WST-1 (Roche, Switzerland) was added to the cells with 100 µL/well after medium change for 4 h incubation at 37 °C. Then the culture medium was transferred from 24-well to 96-well plates and the absorbance was measured with an ELISA reader at 450 nm with a reference wavelength at 630 nm.

2.4. SILAC labeling

All SILAC reagents were from the Pierce™ SILAC Protein Quantitation Kits (Thermo Fisher Scientific Inc, Waltham, MA).

Cells were grown in SILAC "light" (L-lysine and L-arginine) and "heavy" (L-¹³C₆-lysine and L-¹³C₆¹⁵N₄-arginine) conditions for at least five rounds of cell division in SILAC DMEM supplemented with 10% dialyzed fetal bovine serum for complete incorporation of isotope-labeled amino acids. In order to confirm that the SILAC medium has not induced additional effect on the biocompatibility, cells in both "heavy" and "light" medium were examined with an optical microscopy prior to the treatment with materials. Subsequently, the cells in the "heavy" condition were seeded onto cpTi and PEEK disks, whereas the cells in the "light" condition were retained on TCP as controls.

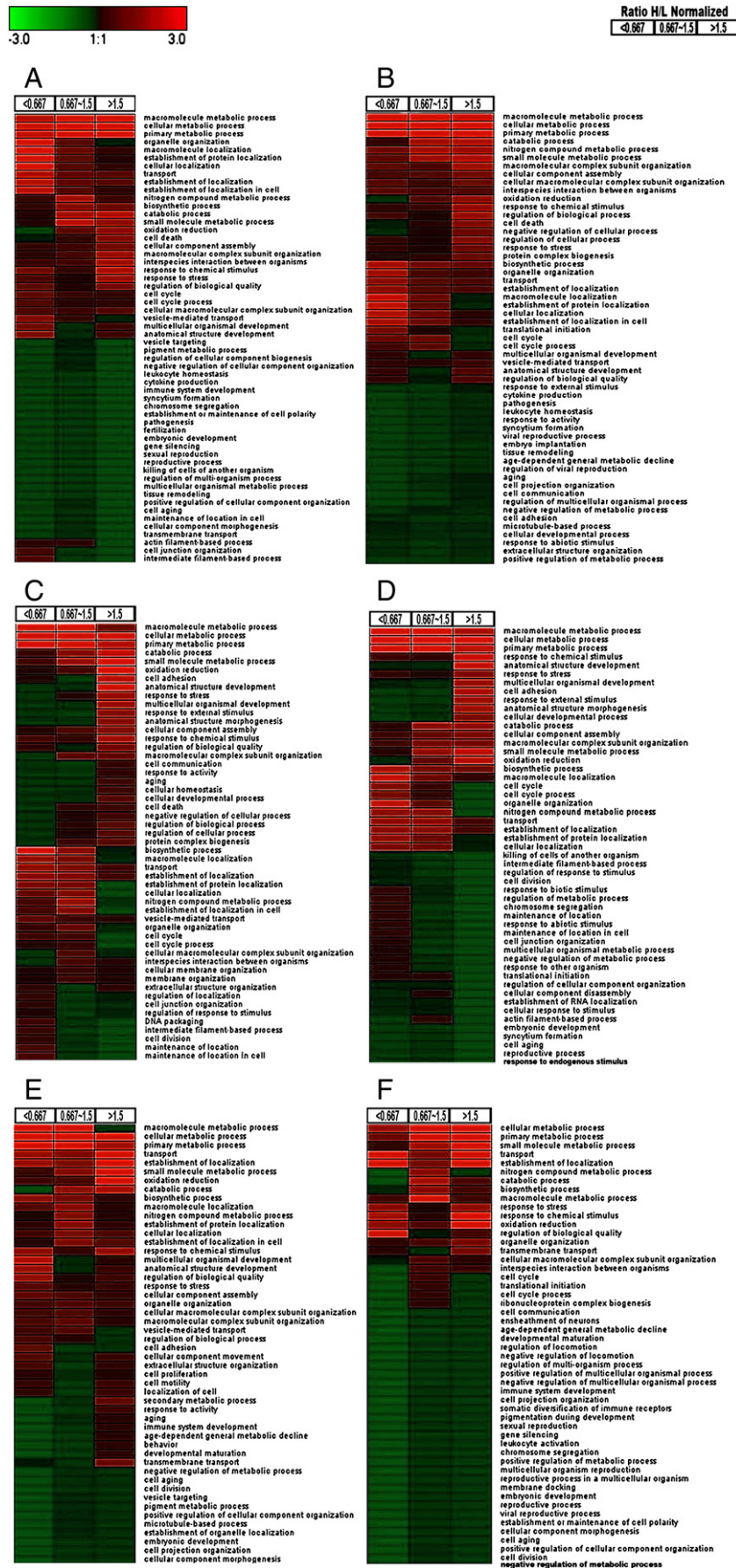
2.5. Protein extraction, separation and in-gel digestion

After 3, 7 and 14 days of culture in SILAC medium, the cells were lysed and harvested in a buffer containing 7 M urea, 2 M thiourea, 4% w/v CHAPS, 65 mM DTT, 1% (v/v) protease inhibitor cocktail (Sigma, USA), and 0.1 volume of the mixture of Deoxyribonuclease I (1 mg/mL) and Ribonuclease A (0.25 mg/mL) at 4 °C for 60 min. The lysates were dissolved with repeated vortex and ultra-sonication, followed by centrifugation at 15,000 g at 4 °C for 30 min to remove insoluble substances. The total protein concentration was determined by the Bradford assay. Proteins from the test groups (cpTi and PEEK) and control group (TCP) were mixed at a ratio of protein amounts at 1:1 for a total of 60 µg proteins. They were then separated by sodium dodecyl sulfate polyacrylamide gel electrophoresis on a 12.5% gel. Gels were fixed and stained with Coomassie Brilliant Blue. Each of the two gel lanes (cpTi/TCP group and PEEK/TCP group) was excised into 15 slices. The slices were then cut into 1 mm³ pieces and destained in 50% acetonitrile with 25 mM ammonium bicarbonate solution, before being dehydrated in 100% acetonitrile and dried. The in-gel proteins were reduced by incubation with 10 mM dithiothreitol for 40 min at 56 °C, followed by alkylation with 55 mM iodoacetamide for 40 min in the dark. After being washed and dehydrated, the proteins were digested with 8 ng/µL sequencing grade trypsin at 37 °C overnight. The peptides were extracted from gel pieces with 0.1% formic acid and 50% acetonitrile for 120 min twice, and the extracts were dried in a vacuum centrifuge.

2.6. LC-MS/MS analysis and data acquisition

Peptides were re-dissolved in 10 µL 0.2% formic acid and injected into a fused silica emitter via auto-sampler with a commercial C₁₈ reverse-phase column (150 mm long, 75 µm inner diameter, packed in-house with C18-AQ 5 µm resin), before being eluted with nano-flow liquid chromatography system (Micro-Tech Scientific, USA). This procedure used a linear gradient from 5% to 30% of acetonitrile in 0.1% formic acid at a constant flow rate of 500 nL/min over 110 min. Eluted peptides were sprayed into a LTQ-Orbitrap mass spectrometer (Thermo Fisher Scientific Inc., USA) via a nano-electrospray ion source.

Fig. 5 – Functional distributions of proteome comparisons revealed by GO biological processes analysis. The color bar upright represents the quantiles. A, C, E: representative functional categories of the cell proteomes in response to cpTi against those in response to TCP on days 3, 7 and 14. B, D, F: representative functional categories of the cell proteomes in response to PEEK against those in response to TCP on days 3, 7 and 14.



The data was acquired in the positive ion mode in a data-dependent mode to automatically switch between the full-scan MS (from m/z 300 to 2000) and the tandem mass spectra (MS/MS) acquisition. The survey spectra were acquired in the Orbitrap with the resolution set to a value of 60,000. Fragmentation in the LTQ was performed by collision-induced dissociation (CID) with 35% normalized collision energy.

Raw MS spectra were processed using the MaxQuant software (version 1.0.12.31) that did peak list generation, quantitation, and data filtration and presentation [10]. MS/MS spectra were searched by Mascot (version 2.2.2, Matrix Science) against the IPI human data base (version 3.24) and the reversed sequences of all proteins. Enzyme specificity was set to trypsin. Carbamidomethylation was set as fixed modification, as well as Lys8 and Arg10 (SILAC label modification). Variable modifications included oxidation (M) and N-acetylation (protein). Maximum two missed cleavages were allowed. Initial mass deviation of precursor ion and fragment ions is up to 10 ppm and 0.5 Da; the minimum required peptide length was set to 6 amino acids. Protein identification required two peptides, one of which had to be unique to the protein group. A false discovery rate (FDR) of 0.01 for proteins and peptides was required. False discovery rate of proteins was the product of the posterior error probability of the contained peptides where only peptides with distinct sequences were taken into account. Posterior error probability for peptides was calculated by recording Mascot score and peptide sequence length-dependent histograms of forward and reverse hits separately. Bayes theorem was then used to derive the probability of a false identification for a given top scoring peptide. False discovery rate was calculated by successively including best scoring peptide hits until the list contained 1% reverse hits. The quantification procedure was described in detail in ref [11].

2.7. Data analysis and interpretation

In the experiment comparing cpTi against TCP (cpTi/TCP group) and that comparing PEEK against TCP (PEEK/TCP group), the quantified proteins were divided into three quantiles corresponding to the cutoffs of 1.50 and 0.667 of the normalized heavy/light ratios. Fold-changes >1.50 were considered as up-regulation, while <0.667 (reciprocal of 1.50)-fold changes were considered as down-regulation. Values between 0.667 and 1.5 indicated no change. The classification and enrichment analysis of different ratio quantiles for the KEGG pathway and for gene ontology (GO) biological process were performed separately by the Genecodis 2 system (<http://genecodis.dacya.ucm.es/>) [12,13], in which the hypergeometric test was employed for enrichment. The categories that were enriched at least in one of the quantiles with a p value less than 0.05 were filtered for hierarchical clustering. The categories without p values after collection in any quantile were provided a very conservative p value of one (in order to analyze all three quantiles and the two test materials equally). This filtered p value matrix was transformed by using the function of $x = -\log_{10}(p \text{ value})$. The x values were transformed to z -scores for each functional category using the transformation $[x - \text{mean}(x)]/\text{sd}(x)$. A hierarchical clustering analysis was performed using the software Genesis (version 1.7.5) [14]. These z -scores obtained above were clustered by one-way hierarchical

clustering, using the “Euclidean distance” as distance function and the “Average Linkage Clustering” method. To understand the interaction of differentially expressed proteins visually, some biological pathways and networks were further analyzed by GenMAPP (<http://www.genmapp.org/>) [15].

2.8. Western blot analysis

Cells were lysed with the same method of 2.4 at each time point. 30 μg proteins were loaded onto 12.5% SDS polyacrylamide gels (SDS-PAGE), separated, and then transferred to PVDF membranes. The membranes were then blocked in 5% skim milk and incubated with primary antibodies against NDRG1, TGF- β 1, ANGPTL4 and GAPDH (Abcam, Cambridge, UK). The blots were developed by chemiluminescence using Amersham ECL reagents (GE Healthcare, Little Chalfont, UK).

2.9. Statistical analysis

Except for KEGG and Gene Ontology enrichment analysis-based hierarchical clustering which used hypergeometric test, all experimental data were expressed as mean \pm standard deviation ($n=6$) and were tested with ANOVA. The level of statistical significance was defined as $p < 0.05$.

3. Results and discussion

3.1. Material characterizations

In our study, both materials went through the same surface polishing process. No significant differences in surface topography (Fig. S1) or surface arithmetic average roughness ($Ra_{\text{cpTi}} = (0.23 \pm 0.06) \mu\text{m}$ and $Ra_{\text{PEEK}} = (0.26 \pm 0.08) \mu\text{m}$, $p = 0.234$) were observed between the surfaces of cpTi and PEEK.

3.2. Cell proliferation assay and morphology observation

The proliferation of cells cultured on both cpTi and PEEK was lower than that on TCP. In addition, the cells on PEEK had significantly lower proliferation than those on cpTi at the two latter time points, especially on day 7 (Fig. 1). The cell morphology of osteoblasts grown on these three different surfaces were similar at all three time points examined, except that cells cultured on cpTi and PEEK extended along the micro-grooves on the surface created by polishing, while the cells cultured on TCP spread randomly (Fig. S2).

3.3. Quantitative proteomic comparison results

In order to characterize the alterations in global protein expression in response to direct contact with cpTi and PEEK, MG-63 cells were labeled and the proteins were quantified following standard SILAC operating procedures (Fig. 2). Fig. S5 shows that the cells cultured in “light” and “heavy” conditions have the same morphology. This indicates that the SILAC medium has not induced additional effect on the biocompatibility of the studied materials due to the existence of the labeling material. Cells labeled with “heavy” ($L\text{-}^{13}\text{C}_6\text{-lysine}$ and $L\text{-}^{13}\text{C}_6^{15}\text{N}_4\text{-arginine}$) amino acids were cultured on cpTi and PEEK disks while cells

with a “light” (L-lysine and L-arginine) label were retained on TCP as controls. Proteins from the test groups (cpTi and PEEK) and control group (TCP) were mixed at a ratio of total protein amounts of 1:1. The protein ratios were normalized to correct for unequal protein amounts to create normalized ratios of heavy/light proteins. Detailed quantitative results at protein level are shown in Tables S1–S2 and peptide level are shown in Tables S5–S6.

Histograms indicating the distribution of fold-changes are shown in Fig. 3. Many proteins showed at least a 1.5-fold difference in expression when grown on cpTi and PEEK compared with TCP. On day 3, the highest frequency around zero (1-fold with least change) was about 200 times the differential distribution. As time in culture increased, the differential distribution became more and more concentrated and the highest frequency reached above 500 in both comparison groups.

3.4. Functional enrichment analysis-based hierarchical clustering

KEGG and GO enrichment analysis-based hierarchical clustering was utilized for data interpretation. The normalized ratios in every section of the comparisons were further classified separately and a hypergeometric test was performed to assess the over-represented categories with reference to the databases of KEGG Pathways (Release 53.0, January 1, 2010) and GO biological processes (GO Annotations Human (EBI), Revision: 1.142). The functional categories were then composed of *p* values. After transformation and clustering, the results were converted to a “heat map”. The representative enriched sections of the categories are shown in Figs. 4–5 (Complete enrichment results made up of *p* values are shown in Figs. S3–S4).

By means of functional classification of related pathways and processes based on the up- or down-regulation of proteins, together with the effect of statistical testing (taking *p* values as input for clustering) and hierarchical clustering with intuitive simplicity, we obtained an unbiased global portrait of representative biological functions. This enables visual interpretation of the functional distribution in terms of aggregate modules on a system level. Many proteins showed altered expression in response to contact with cpTi and PEEK at different time points (Table 1), and the protein expression ratios were distributed over a wide range (Fig. 3). These ratios became more and more concentrated and the frequencies near the zero-point increased dramatically in line with longer contact time with the biomaterials. Similar patterns were also observed in the KEGG and GO

enrichment analyses, which showed that differential enrichment of some categories reverted to control levels with increasing time in culture. These changes revealed the adaptation of cells to their changed environments.

In analysis of the KEGG pathway (Fig. 4), one of the most enriched categories was “ribosome”, which was obviously enriched in both up- and down-regulated categories for both materials on day 3 (Fig. 4 A, B). After 14 days, enrichment of the up-regulated section (>1.5 fold) was disappeared in both groups (Fig. 4 E, F). Alterations in the interfaces between the cells and the substrates would force the cells to produce new proteins and change the expression of some proteins in order to respond and adapt to the new environment. This is reflected in the enrichment of the ribosome, which plays an important part in protein synthesis. However, such responses must be controlled and tightly regulated, and endless proteins synthesis should be prevented. This might be the reason of the disappearance of up-regulation enrichment in both groups with sustained contact.

In both comparison groups, enrichment of the “Glycolysis/Gluconeogenesis” category changed from up-regulation to no change over two weeks of culture. At the same time, the processes of “oxidative phosphorylation”, and “TCA cycle” showed opposite changes, indicating the variation in the energy demands of cells in response to material contact, away from less efficient anaerobic metabolism and toward enhanced oxidative metabolism. Large-scale protein synthesis and modulation requires a great deal of energy for new surface adaptation. As a result, glycometabolism categories (such as the “pentose phosphate pathway” and “fructose and mannose metabolism”) and lipid metabolism categories (such as “fatty acid metabolism” and “fatty acid elongation in mitochondria”) also showed up-regulation enrichment at day 7 (Fig. 4 C and D) and at day 14 in both groups (Fig. 4 E and F). This process was also associated with metabolism in GO biological processes that showed similar patterns. As shown in Fig. 5, the most prominent clusters were related to metabolic processes. Co-enrichment in two or all three sections was observed in some categories. The extent of enrichment of the up-regulated sections was reduced as time in culture increased. “Oxidation reduction” also became more intensely enriched at later time points (Fig. 5 C–F).

As for the KEGG pathway at day 3, several categories related to cell migration, adhesion, and cytoskeletal processes, such as “regulation of the actin cytoskeleton”, “focal adhesion,” and “ECM-receptor interaction”, were enriched in the down-regulation section for both groups, but changed to up-regulation on day 7. In GO biological progress enrichment analysis, “cell adhesion” showed relatively intense enrichment in the up-regulation section on day 7. This indicated that these two bioinert materials which had not undergone surface modification may have worse effects on cell adhesion compared to TCP in the early phase. However, this effect can be improved along with the cells’ adaption to the new surface. Several categories in GO, like “response to chemical stimulus”, “response to stress”, and “negative regulation of cellular processes” were also enriched in the up-regulation sections in the two groups at all three time points. They literally reflect a foreign body response to the inert materials.

Besides the similarities described above, some different processes were found between the two implant materials.

Table 1 – Proteins identified and quantified results of cpTi and PEEK.

		Total protein number	Time points		
			3-day	7-day	14-day
cpTi/TCP	Identified	1582	2074	2150	
	Quantified	1198	1681	1851	
	Up-regulated(ratio \geq 1.5)	249	178	101	
	Down-regulated(ratio \leq 0.667)	148	234	217	
PEEK/TCP	Identified	1961	2207	2171	
	Quantified	1414	1801	1841	
	Up-regulated(ratio \geq 1.5)	279	154	117	
	Down-regulated(ratio \leq 0.667)	426	390	190	

The most prominent diversity was exhibited in KEGG analysis. The category of “aminoacyl-tRNA biosynthesis” and “amino sugar and nucleotide sugar metabolism” were more enriched in the down-regulation section at the first two time points in the PEEK/TCP group than in the cpTi/TCP group (more enriched in the no-change section). The changes in these categories would affect the protein translation process. Additionally, the category of “spliceosome” was enriched mainly in the no-change section in both groups on day 3, but exhibited obvious down-regulation enrichment in the PEEK/TCP group ($p=3.15 \times 10^{-6}$) compared to the cpTi/TCP group ($p=0.004$) on day 7. The spliceosome plays an important role in the splicing process. Processing of pre-mRNAs by RNA splicing is an essential step in the maturation of protein coding RNAs in eukaryotes [16]. To further understand the interaction of differentially expressed proteins about the crucial process of cell viability and proliferation which was related to mRNA transcription, the biological pathway “mRNA processing” was displayed in Fig. 6 by GenMAPP. PEEK/TCP group showed more down-regulated proteins than cpTi/TCP group at day 7. Furthermore, the more obvious enrichment of “cell cycle” and “DNA replication” categories occurred in the down-regulation section especially on day 7 in the PEEK/TCP group. And the up-regulation enrichment of the category of apoptosis on day 14 only appeared in the PEEK/TCP group. These pathways are expected to have a significant effect on cell proliferation. These findings cast light on the mechanism of the more inhibitory effect of PEEK on cell viability compared to cpTi (Fig. 1) at the two later time points.

On day 3, some categories that were related to inflammation and immunity, like “complement and coagulation cascades” and “B cell receptor signaling pathway” [17–19], were more enriched in the cpTi/TCP group than in the PEEK/TCP group. The “MAPK signaling pathway” and “VEGF signaling pathway” categories were both enriched only in the cpTi/TCP group. These changes correlated to inflammatory processes or could be activated in response to pro-inflammatory stimuli [20]. One problem associated with titanium and its alloys (as well as other metal alloys) when used as implants is the transient inflammatory response [21]. Our results confirmed the previously reported results that PEEK was less pro-inflammatory than cpTi [22]. A series of categories such as “Huntington’s disease”, “Parkinson’s disease” and “Alzheimer’s disease”, were more concentrated in the no-change section in the PEEK/TCP group, compared to some degree of enrichment in the up-regulation section in the cpTi/TCP group on day 7. After another week of contact, these categories showed obvious enrichment in the up-regulation section. In the cpTi/TCP group, the up-regulation enrichment was more significant than the no-change enrichment, while the PEEK/TCP group exhibited the opposite pattern, which indicates that PEEK has a reduced correlation to these diseases. (The complete p value information is listed in Tables S3–S4).

In GO enrichment analysis, some important biological progresses for implant materials were not obviously enriched and seen in “heat map”, like “ossification”. But we could still find more obvious down-regulation enrichment in the PEEK/TCP group ($p=0.00159$) compared to the cpTi/TCP group ($p=0.0156$) on day 14 (see Table S4). This indicates that PEEK induces more inhibiting effect to the bone formation related proteins.

The ability to capture these subtle changes by the high sensitivity SILAC coupled proteomics and the way in which information on regulation obtained by this systematic analysis will help to demonstrate the unbiased advantages of proteomic analysis at a global scale.

3.5. Main biological effect of bioinert implant materials to cells

After analyzing systematic functional enrichment, several notable proteins with significant differences at least one time-point were further discussed below. Their expression ratios and changes were showed in Fig. 7. Expression of protein NDRG1 and Angiotensin-related protein 4 were confirmed by Western blot analysis (Fig. 8). Protein NDRG1 is induced by a wide variety of stress and cell growth-regulatory conditions [23]. It is reported to be related to nickel ions. In this study, we found that protein NDRG1 was significantly up-regulated at the first two time-points in response to both metal and polymer materials. Therefore, protein NDRG1 may not have high specificity to nickel and may only serve as a short-term marker of the stress response. Transforming growth factor beta-induced protein ig-h3 (TGFBI) which contains an RGD motif has been shown to interact with different integrins, fibronectin, and collagen to stimulate cell migration [24]. These interactions inhibit cell adhesion. Collagen VI acts as a cell-binding protein and also contains RGD sequences [25]. Both these proteins are related to cell adhesion/migration. The initial high ratios of TGFBI and later up-regulation of Collagen VI were consistent with the KEGG analysis of the regulation of cell adhesion. High mobility group protein B1 (HMGB1) was recently identified as both a danger signal and a potent pro-inflammatory mediator [26]. It was significantly down-regulated in both comparisons except to cpTi at day 7. Ferritin has been reported to possess iron-independent, cytokine like activity to up-regulate the expression of pro-inflammatory mediators [27]. The expression of ferritin was obviously up-regulated at the first two time-points in response to cpTi and PEEK, and more significant to cpTi at day 7. Beta-enolase deficiency is usually considered in the diagnosis of metabolic myopathies due to inherited defects of distal glycolysis [28]. In this study, the ratio of beta-enolase was significantly increased on day 3 in both groups followed by a gradual decrease, suggesting a time-dependent evolution of metabolic adaptation. Angiotensin-related protein 4 (ANGPTL4) has been reported to inhibit cell proliferation, migration, and tubule formation [29]. ANGPTL4 plays an important role in energy metabolism, glucose homeostasis, lipid metabolism, and insulin sensitivity [30]. In our study, ANGPTL4 was significantly up-regulated at the first two time-points, and especially on day 7. These functions were consistent with the cell viability and KEGG analysis results. Combined with the enrichment of GO process “ossification” at day 14, it confirms that in the initial phase, implant material treatment induced striking expression level increases of the angiogenic genes, and they take place ahead of bone events like osseointegration [31].

Each of the proteins described above has various functions. However, they have four functions in common: stress response, cell migration, pro-inflammatory response, and energy metabolism. Interestingly, we found these strongly modulated proteins

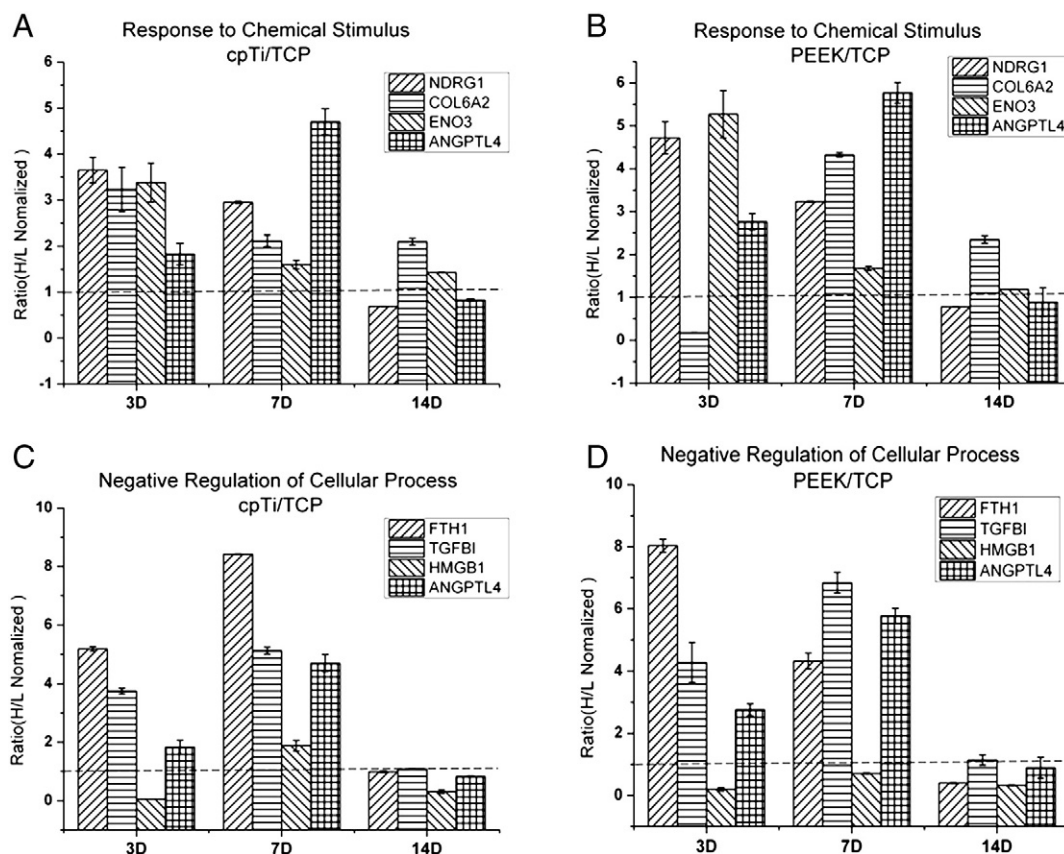


Fig. 7 – The ratios of several significantly differentially expressed proteins which were included in two GO biological process categories: A and B, Response to chemical stimulus (GO:0042221) in the cpTi/TCP and the PEEK/TCP group. C and D, Negative regulation of cellular process (GO:0048523) in the cpTi/TCP and the PEEK/TCP group. NDRG1, TGFBI, ANGPTL4, ENO3, HMGB1, FTH1 and COL6A2 represent protein NDRG1, protein transforming growth factor-beta-induced protein ig-h3, Angiopoietin-related protein 4, beta-enolase, high mobility group protein B1, ferritin heavy chain and collagen alpha-2(VI) chain respectively.

all belong to the GO biological progresses of “response to chemical stimulus” (GO: 0042221) and “negative regulation of cellular process” (GO: 0048523). These proteins exhibited similar variation tendencies to the cpTi/TCP group and PEEK/TCP group (Fig. 7). The meaning of these biological processes may represent the main biological effects at a molecular level as a result of exposure to inert materials.

The ratio distribution of both comparison groups overlapped qualitatively and displayed either close degrees of enrichment or similar fold-changes. Most ratios became concentrated with time of contact. The expressions of the significantly modulated proteins described above were consistent with this regulation. Although they have a different chemical composition, cpTi and PEEK are both inert biomaterials and are usually utilized as foundation materials. From these results, the meaning of “inert material” is better understood at the proteomic level. Both biomaterials could alter the expression of similar types of proteins. The expression changes decreased and became concentrated after a time. Although they are “inert”, the main biological effects caused by these materials still include negative regulation.

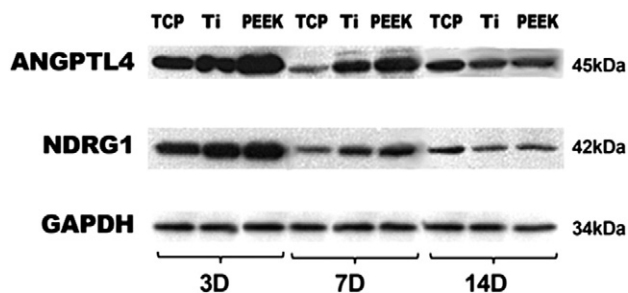


Fig. 8 – Western blot analysis of protein NDRG1, Angiopoietin-related protein 4 and GAPDH for osteoblast cultured on the surface of TCP, cpTi and PEEK for 3, 7 and 14 days.

4. Conclusions

Using SILAC and a systematic data analysis method, we obtained unbiased interpretation of the human osteoblast-like MG-63 cells in response to cpTi and PEEK, two implant materials with different chemical compositions at the molecular level in terms of aggregated functional cluster. Our results revealed the characteristics and dynamic changes of cell adaption to

these common bioinert materials at the quantitative proteomic level, which involves the regulation of biosynthesis and energy metabolism, as well as cell adhesion. Most significantly regulated proteins belonged to the stimulation response and negative regulation processes, which represented the main effects of inert biomaterial treatment on cells. The mechanism of the increased inhibitory effects of PEEK compared to cpTi on cell proliferation occurred through more enrichment of down-regulated proteins in some cellular processes related to transcription, translation and replication of genetic information. For biomaterial-cell interactions, no single action site exists as it does for small molecules, thus material treatment may induce a cooperative response including many proteins, even a group of pathways. This situation requires a global detection and systematic analysis that can make full use of the advantages of proteomics. The systematic comprehension of base inert materials will help to lay a foundation for a better understanding of the biocompatibility of modified implant biomaterials at the global molecular level.

Acknowledgments

This work was supported by grants from the National Key Basic Research Program of China (No. 2007CB936103, 2010CB912203 and 2011CB915504), the National Natural Science Foundation of China (No. 90919023 and 30970652) and the Fundamental Research Funds for the Central Universities.

Appendix A. Supplementary data

Supplementary data to this article can be found online at [doi:10.1016/j.jprot.2012.03.033](https://doi.org/10.1016/j.jprot.2012.03.033).

REFERENCES

- Power KA, Fitzgerald KT, Gallagher WM. Examination of cell–host–biomaterial interactions via high-throughput technologies: a re-appraisal. *Biomaterials* 2010;31:6667–74.
- Xu JL, Khor KA, Sui JJ, Zhang JH, Chen WN. Protein expression profiles in osteoblasts in response to differentially shaped hydroxyapatite nanoparticles. *Biomaterials* 2009;30:5385–91.
- Witzmann F, Monteiroriviere N. Multi-walled carbon nanotube exposure alters protein expression in human keratinocytes. *Nanomedicine* 2006;2:158–68.
- Ong SE, Mann M. Mass spectrometry-based proteomics turns quantitative. *Nat Chem Biol* 2005;1:252–62.
- Lautenschlager EP, MP. Titanium and titanium alloys as dental materials. *Int Dent J* 1993;43:245–53.
- Han C-M, Lee E-J, Kim H-E, Koh Y-H, Kim KN, Ha Y, et al. The electron beam deposition of titanium on polyetheretherketone (PEEK) and the resulting enhanced biological properties. *Biomaterials* 2010;31:3465–70.
- Toth JM, WM, Estes BT, Scifert JL, Seim III HB, Turner AS. Polyetheretherketone as a biomaterial for spinal applications. *Biomaterials* 2006;27:324–34.
- Sagomyants KB, Jarman-Smith ML, Devine JN, Aronow MS, Gronowicz GA. The in vitro response of human osteoblasts to polyetheretherketone (PEEK) substrates compared to commercially pure titanium. *Biomaterials* 2008;29:1563–72.
- Pan Cuiping, CK, Bohl Sebastian, Klingmueller Ursula, Mann Matthias. Comparative proteomic phenotyping of cell lines and primary cells to assess preservation of cell type-specific functions. *Mol Cell Proteomics* 2009;8:443–50.
- Cox J, Matic I, Hilger M, Nagaraj N, Selbach M, Olsen JV, et al. A practical guide to the MaxQuant computational platform for SILAC-based quantitative proteomics. *Nat Protoc* 2009;4:698–705.
- Cox J, Mann M. MaxQuant enables high peptide identification rates, individualized p.p.b.-range mass accuracies and proteome-wide protein quantification. *Nat Biotechnol* 2008;26:1367–72.
- Nogales-Cadenas R, Carmona-Saez P, Vazquez M, Vicente C, Yang X, Tirado F, et al. GeneCodis: interpreting gene lists through enrichment analysis and integration of diverse biological information. *Nucleic Acids Res* 2009;37:W317–22.
- Carmona-Saez P, CM, Tirado F, Carazo JM, Pascual-Montano A. GENECODIS: a web-based tool for finding significant concurrent annotations in gene lists. *Genome Biol* 2007;8:R3.
- Sturn A, Quackenbush J, Trajanoski Z. Genesis: cluster analysis of microarray data. *Bioinformatics* 2002;18:207–8.
- Dahlquist KD, Salomonis N, Vranizan K, Lawlor SC, Conklin BR. GenMAPP, a new tool for viewing and analyzing microarray data on biological pathways. *Nat Genet* 2002;31:19–20.
- Ritchie DB, Schellenberg MJ, MacMillan AM. Spliceosome structure: piece by piece. *Biochim Biophys Acta (BBA) - Gene Regul Mech* 2009;1789:624–33.
- Bhole D, Stahl GL. Therapeutic potential of targeting the complement cascade in critical care medicine. *Crit Care Med* 2003;31:97–104.
- Norris LA. Blood coagulation. *Best Pract Res Clin Obstet Gynaecol* 2003;17:369–83.
- Niir H, Clark EA. Decision making in the immune system: regulation of B-cell fate by antigen-receptor signals. *Nat Rev Immunol* 2002;2:945–56.
- Yang S. Transcriptional regulation by the MAP kinase signaling cascades. *Gene* 2003;320:3–21.
- Hallab NJ. A review of the biologic effects of spine implant debris: fact from fiction. *SAS J* 2009;3:143–60.
- Kurtz SM, Devine JN. PEEK biomaterials in trauma, orthopedic, and spinal implants. *Biomaterials* 2007;28:4845–69.
- Kovacevic Z, Richardson DR. The metastasis suppressor, Ndr-1: a new ally in the fight against cancer. *Carcinogenesis* 2006;27:2355–66.
- Karring Henrik, ZV, Thøgersen Ida B, Hedegaard Chris J, Møller-Pedersen Torben, Kristensen Torsten, et al. Evidence against a blood derived origin for transforming growth factor beta induced protein in corneal disorders caused by mutations in the TGFB1 gene. *Mol Vis* 2007;13:997–1004.
- Chu Mon-Li, T-cP, Conway Dorothy, Kuol Huey-Ju, Glanville Robert W, Timpl Rupert, et al. Sequence analysis of alpha 1(VI) and alpha 2(VI) chains of human type VI collagen reveals internal triplication of globular domains similar to the A domains of von Willebrand factor and two alpha 2(VI) chain variants that differ in the carboxy terminus. *EMBO J* 1989;8:1939–46.
- Erlandsson Harris H, Andersson U. Mini-review: the nuclear protein HMGB1 as a proinflammatory mediator. *Eur J Immunol* 2004;34:1503–12.
- Ruddell RG, Hoang-Le D, Barwood JM, Rutherford PS, Piva TJ, Watters DJ, et al. Ferritin functions as a proinflammatory cytokine via iron-independent protein kinase C zeta/nuclear factor kappaB-regulated signaling in rat hepatic stellate cells. *Hepatology* 2009;49:887–900.
- Comi Giacomo P, Fortunato Francesco, Lucchiarri Sabrina, Bordoni Andreina, Prella Alessandro, Jann Stefano, et al. β -enolase deficiency, a new metabolic myopathy of distal glycolysis. *Ann Neurol* 2001;50:202–7.

-
- [29] Yasuhiro Ito YO, Yasunaga Kunio, Hamada Koichi, Miyata Keishi, Matsumoto Shun-ichiro, Sugano Sumio, et al. Inhibition of angiogenesis and vascular leakiness by angiopoietin-related protein 4. *Cancer Res* 2003;66:51–7.
- [30] Oike Y, Akao M, Yasunaga K, Yamauchi T, Morisada T, Ito Y, et al. Angiopoietin-related growth factor antagonizes obesity and insulin resistance. *Nat Med* 2005;11:400–8.
- [31] Vandamme K, Holy X, Bensidhoum M, Logeart-Avramoglou D, Naert IE, Duyck JA, et al. In vivo molecular evidence of delayed titanium implant osseointegration in compromised bone. *Biomaterials* 2011;32:3547–54.